J|A|C|S ARTICLES

Published on Web 01/12/2009

Probing Single-Molecule Interfacial Electron Transfer Dynamics of Porphyrin on TiO_2 Nanoparticles

Yuanmin Wang, Xuefei Wang, Sujit Kumar Ghosh, and H. Peter Lu*

Bowling Green State University, Center for Photochemical Sciences, Department of Chemistry, Bowling Green, Ohio 43403

Received September 3, 2008; E-mail: hplu@bgsu.edu

Abstract: Single-molecule interfacial electron transfer (ET) dynamics has been studied by using single-molecule fluorescence spectroscopy and microscopic imaging. For a single-molecule zinc-tetra (4-carboxyphenyl) porphyrin (ZnTCPP)/TiO_2 nanoparticle system, the single-molecule fluorescence trajectories show strong fluctuation and blinking between bright and dark states. The intermittency and fluctuation of the single-molecule fluorescence are attributed to the variation of the reactivity of interfacial electron transfer. The nonexponential autocorrelation function and the power-law distribution of the probability density of dark times imply the dynamic and static inhomogeneities of the interfacial ET dynamics. On the basis of the power-law analysis, the variation of single-molecule interfacial ET reactivity is analyzed as a fluctuation according to the Lévy statistics.

Introduction

Interfacial electron transfer (ET) between dye molecules and semiconductors has attracted considerable attention because of the extensive applications in solar energy conversion,[1−7] photocatalysis,[8−11] and molecular devices.[12−15] Interfacial ET typically involve significant inhomogeneous dynamics and complex local environment[3,16−19] that are often difficult to analyze by traditional ensemble-averaged experiments. Single-molecule spectroscopy,[20−28] which is correlated with fluorescence imaging and advanced photon-stamping technique, is capable of probing the complex systems and revealing a real-time landscape of dynamics.

Interfacial ET dynamics between dye and wide band gap semiconductors, such as TiO_2,[3,29−40] SnO_2[41−43] and ZrO_2[42,44−47]

(1) O'Regan, B.; Grätzel, M. *Nature* **1991**, *353*, 737–740.
(2) Frank, A. J.; Kopidakis, N.; van de Lagemaat, J. *Coordin. Chem. Rev.* **2004**, *248*, 1165–1179.
(3) Biju, V.; Micic, M.; Hu, D.; Lu, H. P. *J. Am. Chem. Soc.* **2004**, *126*, 9374–9381.
(4) Li, B.; Zhao, J.; Onda, K.; Jordan, K. D.; Yang, J. L.; Petek, H. *Science* **2006**, *311*, 1436–1440.
(5) Kondov, I.; Čížek, M.; Benesch, C.; Wang, H. B.; Thoss, M. *J. Phys. Chem. C* **2007**, *111*, 11970–11981.
(6) Peter, L. M. *J. Phys. Chem. C* **2007**, *111*, 6601–6612.
(7) Lee, J. K.; Ma, W. L.; Brabec, C. J.; Yuen, J.; Moon, J. S.; Kim, J. Y.; Lee, K.; Bazan, G. C.; Heeger, A. J. *J. Am. Chem. Soc.* **2008**, *130*, 3619–3623.
(8) Fox, M. A.; Dulay, M. T. *Chem. Rev.* **1993**, *93*, 341–357.
(9) Stock, N. L.; Peller, J.; Vinodgopal, K.; Kamat, P. V. *Environ. Sci. Technol.* **2000**, *34*, 1747–1750.
(10) Kamat, P. V. *J. Phys. Chem. C* **2007**, *111*, 2834–2860.
(11) Hoffmann, M. R.; Martin, S. T.; Choi, W. Y.; Bahnemann, D. W. *Chem. Rev.* **1995**, *95*, 69–96.
(12) Joachim, C.; Ratner, M. A. *Proc. Natl. Acad. Sci. U.S.A.* **2005**, *102*, 8801–8808.
(13) Mikaelian, G.; Ogawa, N.; Tu, X. W.; Ho, W. *J. Chem. Phys.* **2006**, *124*, 131101-1–131101-4.
(14) Venkataraman, L.; Klare, J. E.; Nuckolls, C.; Hybertsen, M. S.; Steigerwald, M. L. *Nature* **2006**, *442*, 904–907.
(15) Wang, L.; Liu, L.; Chen, W.; Feng, Y. P.; Wee, A. T. S. *J. Am. Chem. Soc.* **2006**, *128*, 8003–8007.
(16) Novotny, L. *Appl. Phys. Lett.* **1996**, *69*, 3806–3808.
(17) Lu, H. P. *J. Phys. Condens. Matter* **2005**, *17*, R333−R355.
(18) Leite, V. B. P.; Alonso, L. C. P.; Newton, M.; Wang, J. *Phys. Rev. Lett.* **2005**, *95*, 118301-1–118301-4.
(19) Wang, J.; Wolynes, P. *Phys. Rev. Lett.* **1995**, *74*, 4317–4320.
(20) Betzig, E.; Chichester, R. J. *Science* **1993**, *262*, 1422–1425.
(21) Trautman, J. K.; Macklin, J. J.; Brus, L. E.; Betzig, E. *Nature* **1994**, *369*, 40–42.
(22) Xie, X. S.; Dunn, R. C. *Science* **1994**, *265*, 361–364.
(23) Xie, X. S. *Acc. Chem. Res.* **1996**, *29*, 598–606.
(24) Lu, H. P.; Xie, X. S. *Nature* **1997**, *385*, 143–146.
(25) (a) VandenBout, D. A.; Yip, W. T.; Hu, D. H.; Fu, D. K.; Swager, T. M.; Barbara, P. F. *Science* **1997**, *277*, 1074–1077. (b) Palacios, R. E.; Fan, F.-R.; Grey, J. K.; Suk, J.; Bard, A. J.; Barbara, P. F. *Nat. Mater.* **2007**, *6* (9), 680. (c) Bolinger, J.; Lee, K.-J.; Palacios, R. E.; Barbara, P. F. *J. Phys. Chem. C* **2008**, *112*, 18608.
(26) Moerner, W. E.; Orrit, M. *Science* **1999**, *283*, 1670–1676.
(27) (a) Hu, D. H.; Yu, J.; Barbara, P. F. *J. Am. Chem. Soc.* **1999**, *121*, 6936–6937. (b) Palacios, R. E.; Fan, F.-R.; Bard, A. J.; Barbara, P. F. *J. Am. Chem. Soc.* **2006**, *128*, 9028.
(28) Brown, F. L. H. *Phys. Rev. Lett.* **2003**, *90*, 028302-1–028302-4.
(29) Abuabara, S. G.; Rego, L. G.; Batista, V. S. *J. Am. Chem. Soc.* **2005**, *127*, 18234–18242.
(30) De Angelis, F.; Fantacci, S.; Selloni, A.; Nazeeruddin, M. K.; Grätzel, M. *J. Am. Chem. Soc.* **2007**, *129*, 14156–14157.
(31) Duncan, W. R.; Stier, W. M.; Prezhdo, O. V. *J. Am. Chem. Soc.* **2005**, *127*, 7941–7951.
(32) Harris, J. A.; Trotter, K.; Brunschwig, B. S. *J. Phys. Chem. B* **2007**, *111*, 6695–6702.
(33) Kondov, I.; Thoss, M.; Wang, H. *J. Phys. Chem. A* **2006**, *110*, 1364–1374.
(34) (a) Liu, F.; Meyer, G. J. *J. Am. Chem. Soc.* **2005**, *127*, 824–825. (b) Watson, D. F.; Marton, A.; Stux, A. M.; Meyer, G. J. *J. Phys. Chem. B* **2004**, *108*, 11680–11688.
(35) Pan, J.; Benkö, G.; Xu, Y.; Pascher, T.; Sun, L.; Sundström, V.; Polívka, T. *J. Am. Chem. Soc.* **2002**, *124*, 13949–13957.
(36) Ramakrishna, G.; Verma, S.; Jose, D. A.; Kumar, D. K.; Das, A.; Palit, D. K.; Ghosh, H. N. *J. Phys. Chem. B* **2006**, *110*, 9012–9021.
(37) Robel, I.; Kuno, M.; Kamat, P. V. *J. Am. Chem. Soc.* **2007**, *129*, 4136–4137.
(38) Wang, Q.; Campbell, W. M.; Bonfantani, E. E.; Jolley, K. W.; Officer, D. L.; Walsh, P. J.; Gordon, K.; Humphry-Baker, R.; Nazeeruddin, M. K.; Grätzel, M. *J. Phys. Chem. B* **2005**, *109*, 15397–15409.
(39) Wang, L.; Ernstorfer, R.; Willig, F.; May, V. *J. Phys. Chem. B* **2005**, *109*, 9589–9595.

 © 2009 American Chemical Society

have been widely studied. Due to the energy difference between the lowest unoccupied molecular orbital (LUMO) of the dye and the conduction band (or surface states) of the semiconductors, electrons from the excited-state of dye molecules involve forward electron transfer (FET) into the conduction band or the energetically accessible surface states of the semiconductor nanoparticles (NPs) in a time scale ranging from femtoseconds to several hundred picoseconds.[3,5,29,33−36,40,45,46] The injected electrons perform a complex trapping and detrapping, non-Brownian motion and scattering process before recombination with parent cations or diffuse away to generate photovoltaic potential energy.[48,49] These complex physical processes yield a backward electron transfer (BET) process taking a longer time at about subnanoseconds to several milliseconds.[2,3,35,38,40,45,46]Due to the complexity, the BET dynamics have been found having complex kinetics of single exponential,[50] multiexponential,[36,37,51−58] and stretched exponential.[35,59−65] For efficient dye-sensitized solar cells, fast electron injection and diffusion toward metal electrode, but not for carrier recombination, are desirable. A molecule-level understanding of interfacial ET dynamics is essential for surface chemistry, catalysis, and solar energy science.

In our previous reports, the fluorescence fluctuation dynamics for Coumarin 343 (or Cresyl Violet)/TiO_2 systems were found to be inhomogeneous from molecule to molecule and from time to time, showing significant static and dynamic disorders in the interfacial ET reaction.[3] The origin of the fluorescence fluctuation was attributed to interfacial ET reactivity fluctuation and intermittency at the single molecule/TiO_2 nanoparticle interfaces. In this work, real-time interfacial ET dynamics have been studied based on single-molecule zinc-tetra (4-carboxyphenyl) porphyrin (ZnTCPP)/TiO_2 nanoparticle system by using single-molecule fluorescence imaging and photon-stamping technique. The energy difference (ΔE) between LUMO of ZnTCPP (3.4 $\pm$ 0.2 eV) and the conduction band of TiO_2 (4.4 $\pm$ 0.2 eV) makes charge injection efficient at the ZnTCPP/TiO_2 interface.[66] Ensemble experiments indicate that the electron injection dynamics is multiexponential and ultrafast,[62] as fast as: (i) less than 100 fs (injection yield, 0.37); (ii) 1.1 $\pm$ 0.4 ps (0.12); or (iii) 8.5 $\pm$ 2 ps (0.51). Under a visible light illumination, photocurrent measurements indicate that a high photon-to-current conversion efficiency can be obtained for the ZnTCPP/TiO_2 system.[67] Therefore, we select this system as a model system to probe the inhomogeneous properties that is critical for a mechanistic understanding of fundamental interfacial electron transfer dynamics by using single-molecule spectroscopy approaches. Combining statistical analysis and single-molecule fluorescence spectroscopy, we demonstrate a characterization of the reactivity fluctuation and inhomogeneity of the interfacial electron transfer dynamics in ZnTCPP/TiO_2 nanoparticles.

Experimental Section

Materials and Sample Preparation. Ethanol and poly(methylmethacrylate) (PMMA) (MW 15000) were purchased from Aldrich, and Dichloromethane and ZnTCPP were purchased from EMD chemicals and Frontier Scientific, respectively. All the chemicals were used as received. TiO_2 nanoparticles were prepared using titanium isopropoxide as precursor according to a literature protocol.[68] The average size of the TiO_2 nanoparticles was about 10 to 15 nm, as determined by AFM. Sample preparations for the single-molecule experiments are similar to our previous procedure.[3] Twenty-five microliters of 0.1 nM ZnTCPP in ethanol solution was first spin-coated to a clean coverslip (Fisher, 18 mm $\times$ 18 mm, thickness $\sim$170 μm) at 3000 rpm and overlaid by spin-coating 50 μL PMMA (in CH_2Cl_2, 1 mg/mL). For a control experiment, 50 μL TiO_2 NP solution was first spin-coated on the coverslip and then overlaid by 0.1 nM ZnTCPP and PMMA film.

Single-molecule Fluorescence Spectroscopy and Imaging. Single-molecule fluorescence spectroscopy and imaging were recorded by Axiovert 135 inverted scanning confocal microscope, equipped with a 100 $\times$ 1.3 NA oil immersion objective (Zeiss FLUAR). A continuous-wave (CW) laser (532 nm, CL-2000 diode pumped crystal laser, CrystaLaser) was used to pump the sample at about 200 nW. A beam splitter Z532rdc (Chroma) was used to reflect the excitation light into the objective. The emission light passed through the emission filter HQ545lp (Chroma, for ZnTCPP, the emission wavelength typically ranges from 570 to 750 nm) and collected by a single-photoncounting avalanche photodiode (APD) detector (Perkin-Elmer SPCMAQR-14). Photon-stamping data was recorded by a time-correlated single photon counting (TCSPC) system (SPC-830, Becker & Hickl GmbH) in a FIFO mode. For the single-molecule polarization experiment, a half-wave plate was rotated at a fixed frequency to change the polarization angle of the excitation laser beam. The time-resolved control experiment was

(40) She, C.; Guo, J.; Irle, S.; Morokuma, K.; Mohler, D. L.; Zabri, H.; Odobel, F.; Youm, K. T.; Liu, F.; Hupp, J. T.; Lian, T. *J. Phys. Chem. A* **2007**, *111*, 6832–6842.
(41) Fukai, Y.; Kondo, Y.; Mori, S.; Suzuki, E. *Electrochem. Commun.* **2007**, *9*, 1439–1443.
(42) Kay, A.; Grätzel, M. *Chem. Mater.* **2002**, *14*, 2930–2935.
(43) Green, A. N. M.; Palomares, E.; Haque, S. A.; Kroon, J. M.; Durrant, J. R. *J. Phys. Chem. B* **2005**, *109*, 12525–12533.
(44) Rochford, J.; Chu, D.; Hagfeldt, A.; Galoppini, E. *J. Am. Chem. Soc.* **2007**, *129*, 4655–4665.
(45) Matylitsky, V. V.; Lenz, M. O.; Wachtveitl, J. *J. Phys. Chem. B* **2006**, *110*, 8372–8379.
(46) Ramakrishna, G.; Singh, A. K.; Palit, D. K.; Ghosh, H. N. *J. Phys. Chem. B* **2004**, *108*, 4775–4783.
(47) Ramakrishna, G.; Singh, A. K.; Palit, D. K.; Ghosh, H. N. *J. Phys. Chem. B* **2004**, *108*, 12489–12496.
(48) deJongh, P. E.; Vanmaekelbergh, D. *Phys. Rev. Lett.* **1996**, *77*, 3427–3430.
(49) Klafter, J.; Sokolov, I. M. *Phys. World* **2005**, *18*, 29–32.
(50) Martini, I.; Hodak, J.; Hartland, G. V.; Kamat, P. V. *J. Chem. Phys.* **1997**, *107*, 8064–8072.
(51) Vrachnou, E.; Vlachopoulos, N.; Grätzel, M. *J. Chem. Soc., Chem. Commun.* **1987**, 868–870.
(52) Lu, H.; Prieskorn, J. N.; Hupp, J. T. *J. Am. Chem. Soc.* **1993**, *115*, 4927–4928.
(53) Liu, D.; Fessenden, R. W.; Hug, G. L.; Kamat, P. V. *J. Phys. Chem. B* **1997**, *101*, 2583–2590.
(54) Ghosh, H. N.; Asbury, J. B.; Weng, Y. X.; Lian, T. Q. *J. Phys. Chem. B* **1998**, *102*, 10208–10215.
(55) Ellingson, R. J.; Asbury, J. B.; Ferrere, S.; Ghosh, H. N.; Sprague, J. R.; Lian, T. Q.; Nozik, A. J. *J. Phys. Chem. B* **1998**, *102*, 6455–6458.
(56) Haque, S. A.; Tachibana, Y.; Klug, D. R.; Durrant, J. R. *J. Phys. Chem. B* **1998**, *102*, 1745–1749.
(57) Ghosh, H. N. *J. Phys. Chem. B* **1999**, *103*, 10382–10387.
(58) Weng, Y. X.; Wang, Y. Q.; Asbury, J. B.; Ghosh, H. N.; Lian, T. Q. *J. Phys. Chem. B* **2000**, *104*, 93–104.
(59) Nelson, J. *Phys. Rev. B* **1999**, *59*, 15374–15380.
(60) Nelson, J.; Chandler, R. E. *Coordin. Chem. Rev.* **2004**, *248*, 1181–1194.
(61) Nelson, J.; Haque, S. A.; Klug, D. R.; Durrant, J. R. *Phys. Rev. B* **2001**, *63*, 205321-1–205321-9.
(62) Trachibana, Y.; Haque, S. A.; Mercer, I. P.; Durrant, J. R.; Klug, D. R. *J. Phys. Chem. B* **2000**, *104*, 1198–1205.
(63) Benkö, G.; Hilgendorff, M.; Yartsev, A. P.; Sundström, V. *J. Phys. Chem. B* **2001**, *105*, 967–974.
(64) Huber, R.; Sporlein, S.; Moser, J. E.; Grätzel, M.; Wachtveitl, J. *J. Phys. Chem. B* **2000**, *104*, 8995–9003.
(65) Huber, R.; Moser, J. E.; Grätzel, M.; Wachtveitl, *J. Chem. Phys.* **2002**, *285*, 39–45.
(66) Wienke, J.; Schaafsma, T. J.; Goossens, A. *J. Phys. Chem. B* **1999**, *103*, 2702–2708.
(67) Boschloo, G. K.; Goossens, A. *J. Phys. Chem.* **1996**, *100*, 19489–19494.
(68) Duonghong, D.; Borgarello, E.; Grätzel, M. *J. Am. Chem. Soc.* **1981**, *103*, 4685–4690.

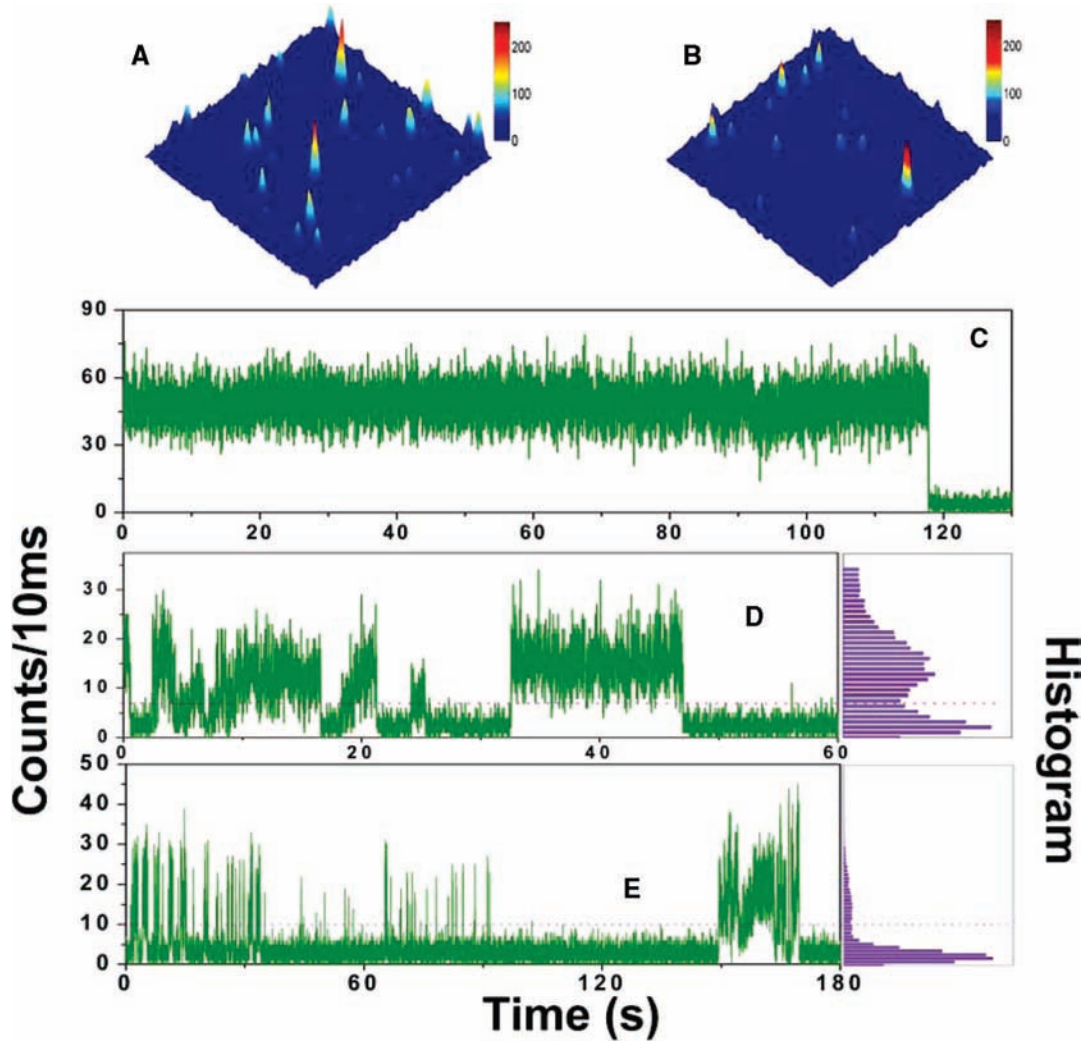

Figure 1. (A and B) 3-Dimension optical images for single ZnTCPP molecules on a cover glass and a TiO_2 nanoparticle covered surface. Size: 10 μm × 10 μm. A typical single-molecule fluorescence emission trajectory of ZnTCPP on a cover glass surface is shown in (C). (D and E) Typical single-molecule fluorescence emission trajectories of ZnTCPP on TiO_2 NP surface. The binning time is 10 ms. Histograms of the emission intensity are given to determine the threshold for dark states and bright states.

performed by a picosecond pulse laser (532 nm, Coherent Antares, YAG) with a repetition frequency of 76 MHz.

Results and Discussion

Figure 1A and B are the optical images for single ZnTCPP molecules on a cover glass and a TiO_2 nanoparticle covered surface, respectively. Figure 1D and E show the typical single-molecule fluorescence emission trajectories for ZnTCPP on TiO_2 NP surface (the binning time is 10 ms). Comparing the continuous emission on the glass surface in Figure 1C, both trajectories show strong fluctuation with dark time ranging from subseconds to seconds.

We have identified that the single-molecule fluorescence intensity fluctuation is not due to triplet state or single-molecule rotational or translational motions during the measurements. The triplet state lifetime of the dye ZnTCPP is about 1.6 ms[69] and hence, the triplet blinking is not responsible for the long dark times (Figure 1D and E). Moreover, we have performed a single-molecule polarization experiment for single-molecule ZnTCPP on TiO_2 NP surface to check whether the fluorescence fluctuation is due to molecule rotation or translation motions.[25,27,70,71] Figure 2A shows the fluorescence fluctuation from time to time and under a deep-sine modulation as the laser polarization is modulated by a half-wave plate rotation at $\sim$ 0.2 Hz. This result indicates that the single molecule fluorescence is from a single transition dipole and the phase represents the orientation of the transition dipole. We analyzed the phase of two periods 1 and 2 and found they remained the same even after a few fluorescence intensity fluctuations (Figure 2B and C), which suggests that the orientation of the single molecule transition dipole has not changed during the measurement. Specifically, the single molecule maintains its transition dipole orientation through a number of fluorescence intensity fluctuations. Different from periods 1 and 2, both 3 and 4 involve in a deep intensity dip in their phase but the molecule still holds the phase after the dip. This result suggests that the transition dipole orientation of the single molecule ZnTCPP does not change significantly during the measurement, and the fluctuation of

(69) Kalyanasundaram, K.; Vlachopoulos, N.; Krishnan, V.; Monnier, A.; Grätzel, M. *J. Phys. Chem.* **1987**, *91*, 2342–2347.
(70) Biju, V. P.; Ye, J. Y.; Ishikawa, M. *J. Phys. Chem. B* **2003**, *107*, 10729–10735.
(71) Forster, M.; Thomsson, D.; Hania, P. R.; Scheblykin, I. G. *Phys. Chem. Chem. Phys.* **2007**, *9*, 761–766.

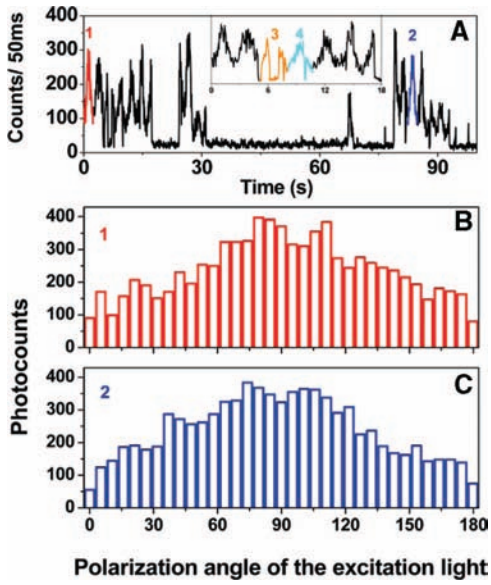

Figure 2. Single-molecule fluorescence polarization profile for ZnTCPP on TiO_2 NP surface. (A) Single-molecule fluorescence trajectory with deep sine-modulation. Two typical sine-modulated periods 1 and 2 are specified. Part of the trajectory from 0 to 18 s is zoomed in and inserted, which highlights two special periods 3 and 4. (B and C) Photocounts-phase relationship for period 1 and 2 that is specified in (A).

fluorescence trajectory is not due to single molecule rotation or translation motions. On the basis of above discussion, we conclude that the dark state in the fluorescence trajectory is due to ET process with high activity quenching the fluorescence, and the bright state is due to natural fluorescence emission cycles from $S_1 \rightarrow S_0$ and low activity in ET process. This conclusion is consistent with our reported findings on single-molecule interfacial electron transfer of Coumarin 343/TiO_2 and Cresyl Violet/TiO_2 systems.[3]

To further prove our attribution of that the single-molecule fluorescence fluctuation is due to the ET reactivity fluctuation, we have measured the single-molecule fluorescence lifetimes by single-molecule time-resolved fluorescence photon-stamping experiments.[3] In a single-molecule photon-stamping measurement, the chronic arrival time and the delay time from the laser pulse excitation are recorded for each detected photon (Figure 3A and C). Each data point in Figure 3A and C represents a detected photon with recorded delay time (y-axes) and chronic arrival time (x-axes). A distribution along the y-axes gives a typical single-molecule fluorescence decay curve, and a binning along the x-axes gives a typical single-molecule fluorescence intensity trajectory. We analyzed the single-molecule fluorescence lifetime for both the higher-level emission intensity and lower-level emission intensity. The emission intensity in a trajectory is separated to higher level and lower level based on a threshold of 20 photon-counts/10 ms (Figure 3B). In Figure 3A and C, two dimension photon-stamping data, including arriving time and delay time for each photon, are displayed for a typical bright state (in "pink", 0.34−0.77 s) and a dark state (in "purple", 15.73−17.00 s). Though the lifetimes of these two typical blinking events are different, for whole trajectory, the lifetimes for high-level and low-level emission are very close (Figure 3D), and only the pre-exponential amplitudes are different. This means the fluorescence intensity is determined by the fraction of time in which the interfacial ET occurs but not the ET rate. The above lifetime analysis also is consistent with the single-molecule lifetime fluctuating trajectory (Figure

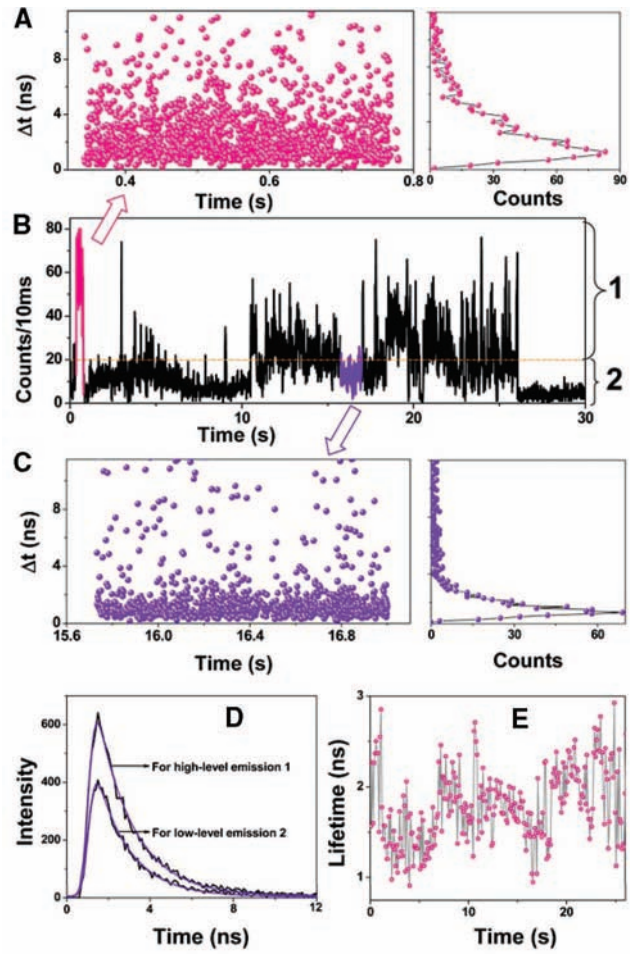

Figure 3. Single-molecule fluorescence decay profile of ZnTCPP on TiO_2 NP surface. Photon-stamping data (including arriving time and delay time for each photon) for typical high emission intensity state (in pink) and low emission intensity state (in purple) are displayed in (A) and (C), respectively. (B) Using 20 photocounts/10 ms as threshold, the emission trajectory is separated to higher level (1) and lower level (2) periods. In (D), fluorescence decay profile for duration 1 and 2 are shown, and the decay times are 1.75 and 1.6 ns, respectively. (E) Single-molecule lifetime fluctuating trajectory of the same molecule from 0 to 26 s.

3E, the same single molecule), which shows fluctuation in a typical range of 1.2 to 2.5 ns. The nanosecond fluctuating amplitude in lifetime trajectory and the strong fluctuation of fluorescence trajectory imply that though the ultrafast FET can not be directly time-resolved by single molecule experiment, the ET reactivity can be reflected by the fluorescence fluctuation. With ET reactivity fluctuating, fluorescence can show dramatic fluctuations and give bright and dark states. However, averagely, the range of the lifetime changes does not suggest the redox state change of the dye molecules, that is, the detected photons are all from the neutral dye molecules of ZnTCPP but not from its oxidized state $ZnTCPP^+$.

Therefore, for ZnTCPP/TiO_2 system, although ET rate is ultrafast in average, the fluorescence is not completely quenched. With the ET reactivity fluctuating from time to time, the individual molecules show fluorescence blinking and they are still observable in the single-molecule imaging at a single photon counting sensitivity.[3] The ET activity is intermittent in nature and does not always dominate the excited state process of the ZnTCPP/TiO_2 system.

The results shown in Figure 3 also suggests that the fluorescence intensity blinking behavior is not due to the

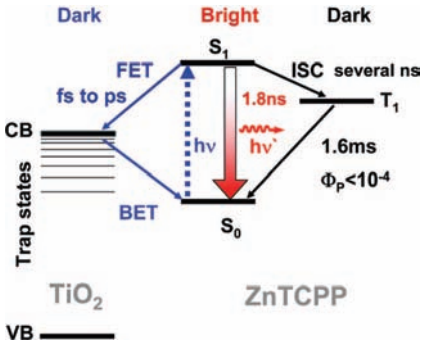

Figure 4. Schematic presentation of energy levels and basic photoinduced process in ZnTCPP/TiO_2 system. CB: conduction band; VB: valence band; FET: forward electron transfer; BET: Backward electron transfer; ISC: intersystem crossing. The dark state on the left is due to that the high ET reactivity quenches the photon emission and the dark state on the right is due to the triplet state of ZnTCPP.

individual event of interfacial ET at subsecond to second time scale associated with detected ZnTCPP state (high fluorescence intensity) and the nonfluorescent or low fluorescent cation oxidized state of ZnTCPP. This is because that the fluorescence lifetime of reduced and oxidized states of single-molecule ZnTCPP should be different significantly, that is, the reduced ZnTCPP fluorescence lifetime is at ns time scale, and the oxidized ZnTCPP cation fluorescence lifetime is at subns to ps time scales. Our control experiments support the conclusion that (1) the single-molecule interfacial electron transfer is ultrafast and not directly time-resolved by our single-molecule photon-stamping measurements; (2) the single-molecule fluorescence intensity fluctuation reflects the single-molecule interfacial electron transfer reactivity fluctuation; (3) when the interfacial electron transfer activity is low, the $S_1 \rightarrow S_0$ radiative emission dominates the signal, and the detected fluorescence intensity is high giving the bright states; (4) whereas, when the interfacial electron transfer activity is high, the electron transfer quenches the $S_1 \rightarrow S_0$ radiative transition, and the detected fluorescence intensity is low giving the dark states. Therefore, (5) the variations of the dark times represent the single-molecule ET reactivity fluctuation; statistically, a longer dark time represents a higher reactivity, and vise versa.

The molecular fluorescence intensity is typically characterized by the fluorescence quantum yield (Q) of the molecules. The value of Q is determined by the ratio of the number of emission photons to the number of excitation photons absorbed. Since the intensity of the CW laser is stable and has almost no drift with time, the excitation photon flux is thereby held stable. Furthermore, the rotation motions of ZnTCPP molecules are rare events within seconds as we have shown (Figure 2), the absorbed photon number is also held stable. Therefore, the single-molecule fluorescence intensity fluctuation, reflected by Q value fluctuation, is due to the emission photon number density fluctuation. Once an excitation photon is absorbed, a single molecule ZnTCPP is excited from S_0 ground-state to the S_1 excited state (Figure 4). The probability of an emission transition from the S_1 excited-state depends on both radiative decay rate constant k_{rad} and nonradiative decay rate constant, k_{nr}, and is given by the relation, $Q = k_{rad}/(k_{rad} + k_{nr})$. If there is no nonradiative decay process ($k_{nr} = 0$) or the nonradiative decay is much slower than the radiative decay ($k_{nr} \ll k_{rad}$), then the $Q = 1$ and the chromophore is bright. If the nonradiative decay is much faster, then the $Q \rightarrow 0$ and the chromophore is dark. Since there is always a nonradiative decay process, and the decay time can be comparable to the radiative decay time, the Q has a finite value between 0 and 1. In a ZnTCPP/TiO_2 nanoparticle system, the k_{rad} is the reciprocal fluorescence lifetime of ns, and k_{nr} is dominated by FET time of fs to ps as both the internal conversion from S_1 to S_0 (ns$-\mu$s) and the intersystem cross from S_1 to T_1 state (several ns) are much slower (Figure 4). The natural fluorescence lifetime is unlikely to fluctuate at ms to seconds under the single-molecule experimental condition; therefore, it is the k_{nr} fluctuation that contributes to the Q fluctuation which in turn contributes to the fluorescence intensity fluctuation (Figure 1).

It is still not technically possible to measure the subps and fs single-molecule electron transfer dynamics directly, although measurements of the ultrafast single-molecule excited-state dynamics has been demonstrated.[73] In our single-molecule fluorescence spectroscopy experiments, what has been measured is the nanosecond emission photons from the $S_1 \rightarrow S_0$ radiative transition, which is related to the quantum efficiency of the excited-state involving in FET as a dominated nonradiative transition, radiative transition, and intersystem cross transition from the singlet S_1 excited-state to the triplet state (Figure 4). In other words, it is the $S_1 \rightarrow S_0$ nanosecond transition that serves as a clock to regulate the decay pathway of the excited-state of ZnTCPP: the FET time apparently fluctuates in a wide time scale from fs to ns or even slower. This is because that if the FET as a nonradiative decay is constant in a fs to ps time scale, the excited-state radiative emission efficiency at ns time scale should be as low as 10^{-3} to 10^{-6}, and the single molecules should be essentially nonfluorescent or not observable by photon detection. However, we have observed that the single-molecule fluorescence intensity is blinking between the dark states and bright states. When the nonradiative FET process is much faster than the nanosecond radiative decay, the single molecule is dark; when the nonradiative FET process is much slower than the nanosecond radiative decay, the single-molecule is bright; when the nonradiative FET time is comparable to the nanosecond radiative decay, the single-molecule fluorescence state is in between bright and dark states. The comparative nonradiative and radiative decay processes determined the fate of the excited states, and in turn determined the brightness of the single molecules. The fluctuation of the single-molecule emission intensity is a reflection of the rate fluctuation of the nonradiative FET process; and the fluctuation of the FET dynamics is practically probed by the nanosecond radiative decay process in determining the fluorescence quantum efficiency.

To analyze the single-molecule interfacial electron transfer dynamics that is associated with the fluctuation of the single-molecule fluorescence trajectories, we have performed statistical analysis on the stochastic durations of the dark states in which the high ET activity takes place. For a single-molecule fluorescence trajectory, a histogram of emission intensity is first constructed and then a threshold is determined (Figure 1D and 1E). The time durations of the dark states or bright states are then obtained. Figure 5A and B show the distributions of the time durations of the dark states for a single molecule (shown in Figure 1D) and 29 molecules, respectively. The duration of the dark states spans a broad range from subseconds to seconds. It is interesting that, for the single molecules, non-Poisson behavior is observed

(72) Lu, H. P.; Xie, X. S. *J. Phys. Chem. B* **1997**, *101*, 2753–2757.

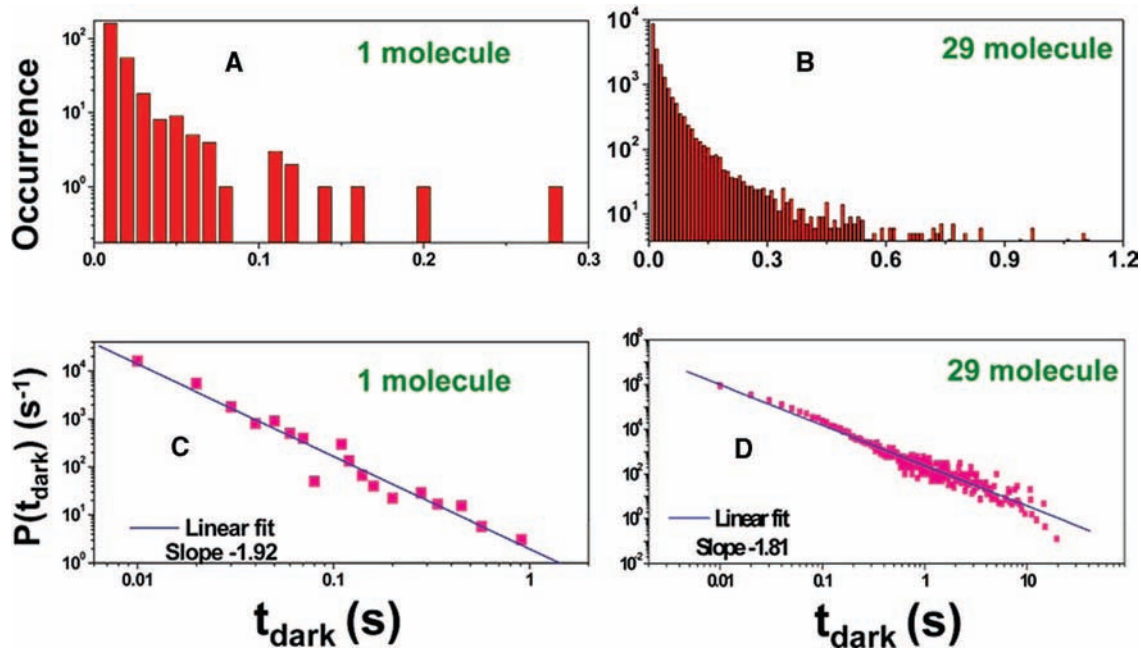

Figure 5. Distributions of occurrence (A and B) and probability density (C and D) of dark state for 1 molecule and 29 molecules. In (A) and (B), the occurrence and dark time are plotted in a semilog to linear scale. There are about 240 and 20K dark states recorded for single molecule (A) and 29 molecules (B), respectively.

evidenced by a nonexponential dark time distributions shown in Figure 5A and 5B. This non-Poisson dark-time distribution suggests that the intrinsic physical mechanism is not originated from a single Poisson event under an exponential rate dynamics, which reflects that the interfacial ET involves complex rate process that cannot be defined by a static rate constant and the rate changes from time to time. This fluctuation behavior has been characterized as dynamic disorder,[3,18,72,74,75]which is beyond the conventional scope of chemical kinetics.

To analyze the ET reactivity fluctuation dynamics associated with the non-Poisson dark time distributions, we have constructed the probability density[76] distributions of the dark states ($P(t_{dark})$ = Occurrence(t)/Δt). Each data point of the histogram is weighted by the average time between nearest neighbor events. The calculated log−log plots (Figure 5C and 5D) of the single-molecule dark-time probability density distributions show typical power-law behavior, which can be mathematically described as $P(t_{dark}) \propto t_{dark}^{-m_{dark}}$. This power-law kinetics quantitatively demonstrates that the dark time probability density distributions are nonexponential and should correspond to non-Poisson dynamics associated with dynamically inhomogeneous ET activity, that is, the ET reaction activity fluctuates from time to time. Power-law behaviors have been extensively investigated in emission blinking dynamics of quantum dots and other single emitters.[76−80] Distributed-traps model and diffusion controlled models have been proposed to rationalize the power-law behavior of quantum dots.[81,82] The former model proposed the quantum dots enter dark state once it loses an electron into the surface traps and become bright again after a nonradiative Auger recombination. The latter model suggests the blinking is controlled by the diffusion of the energy of electron or trap state, and the model agrees well with the experimental results. For the power-law behavior in single molecule blinking, power-law-distributed dark states are found to be the main pathway of photobleach for single organic molecules,[83] and it has been suggested that the power-law blinking of organic molecules seems to require dynamic disorder dynamics.[84] Power-law dynamics has also been observed existing in the vibrational mode fluctuation of single protoporphyrin IX (FePP) molecule from surface-enhanced Raman scattering.[85] Connected with experiment, the origin of power-law distribution in single-molecule conformation dynamics has been theoretically studied.[79,80] In our experiment, the power-law statistical behavior is intrinsically determined by the interfacial ET dynamics. For ZnTCPP/TiO_2 system, the power-law behavior reflects the disorder

(73) Hernando, J.; van Dijk, E. M. H. P.; Hoogenboom, J. P.; García-López, J. J.; Reinhoudt, D. N.; Crego-Calama, M.; García-Parajó, M. F.; van Hulst, N. F *Phys. Rev. Lett.* **2006**, *97*, 216403-1–216403-4.
(74) Holman, M. W.; Liu, R. C.; Adams, D. M. *J. Am. Chem. Soc.* **2003**, *125*, 12649–12654.
(75) (a) Issac, A.; Jin, S. Y.; Lian, T. Q. *J. Am. Chem. Soc.* **2008**, *130*, 11280–11281. (b) Cui, S. C.; Tachikawa, T.; Fujitsuka, M.; Majima, T. *J. Phys. Chem. C* **2008**, *112*, 19625–19634. (c) Xu, W.; Kong, J. S.; Yeh, Y.-T. E.; Chen, P. *Nat. Mater.* **2008**, *7*, 992–996.
(76) Kuno, M.; Fromm, D. P.; Hamann, H. F.; Gallagher, A.; Nesbitt, D. J. *J. Chem. Phys.* **2001**, *115*, 1028–1040.
(77) Shimizu, K. T.; Neuhauser, R. G.; Leatherdale, C. A.; Empedocles, S. A.; Woo, W. K.; Bawendi, M. G. *Phys. Rev. B* **2001**, *63*, 205316-1–205316-5.
(78) Hoogenboom, J. P.; Hernando, J.; van Dijk, E. M. H. R.; van Hulst, N. F.; García-Parajó, M. F. *Chemphyschem* **2007**, *8*, 823–833.
(79) Wang, J.; Xu, L.; Xue, K.; Wang, E. *Chem. Phys. Lett.* **2008**, *463*, 405–409.
(80) Lee, C. L.; Stell, G.; Wang, J. *J. Chem. Phys.* **2003**, *118*, 959–968.
(81) Efros, A. L.; Rosen, M. *Phys. Rev. Lett.* **1997**, *78*, 1110–1113.
(82) Pelton, M.; Smith, G.; Scherer, N. F.; Marcus, R. A. *Proc. Natl. Acad. Sci. U.S.A.* **2007**, *104*, 14249–14254.
(83) Hoogenboom, J. P.; van Dijk, E. M.; Hernando, J.; van Hulst, N. F.; Garcia-Parajo, M. F. *Phys. Rev. Lett.* **2005**, *95*, 097401-1–097401-4.
(84) Cichos, F.; von Borczyskowski, C.; Orrit, M. *Curr. Opin. Colloid Interface Sci.* **2007**, *12*, 272–284.
(85) Bizzarri, A. R.; Cannistraro, S. *Phys. Rev. Lett.* **2005**, *94*, 068303-1–068303-4.

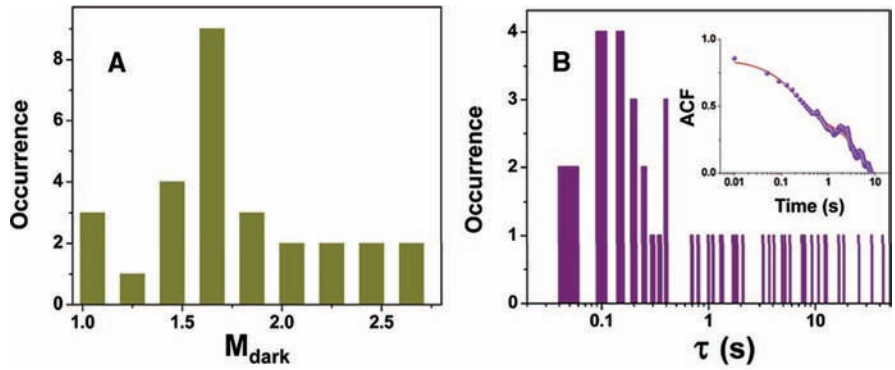

Figure 6. (A) Histogram of power-law exponents for 28 ZnTCPP molecules. (B) Histogram of fluctuation times derived from the autocorrelation function of the fluorescence intensity for 29 ZnTCPP molecules. (Inset) Typical nonexponential autocorrelation function calculated from a single-molecule fluorescence intensity time trajectory. For autocorrelation function of emission intensity, $1/\tau$ represents the fluctuation rate, that is, interfacial ET reactivity fluctuation rate in the ZnTCPP/TiO_2 system.

of the ET reactivity, and the power exponent m_{dark} represents nonexponential distribution nature of the probability of the dark times.

We have calculated the power exponents, m_{dark}, for 28 molecules and obtained a distribution of m_{dark} (Figure 6A). The value ranges from 1.02 to 2.68, which reflects the inhomogeneity of the ET activity fluctuation from molecule to molecule. The mean value of the power exponents $\langle m_{dark} \rangle$ is 1.79. To further understand the ET reactivity fluctuation and the dark-state properties, we calculated the autocorrelation functions of the single-molecule fluorescence intensity trajectories. Most of the autocorrelation functions show nonexponential decays, which is consistent with our previous findings on single-molecule Coumarin 343/TiO_2 and Cresyl Violet/TiO_2 interfacial ET dynamics.[3] The nonexponential autocorrelation function indicates the dynamic disorder of the interfacial ET reactivity, that is, the reactivity fluctuation rate changes from time to time during a single-molecule measurement. We analyzed the autocorrelation functions by biexponential fitting with a wide range of decay time (τ) from milliseconds to seconds for 29 molecules (Figure 6B). Figure 6 shows that a longer time scale τ tends to associate with more disorder of the fluctuation dynamics.

Both the autocorrelation function decay time τ and the power-law exponent, m_{dark} are critical factors characterizing the interfacial ET reactivity fluctuation dynamics. These two parameters correspond to the basic properties of single-molecule fluorescence fluctuations. The autocorrelation function fluctuation time, τ represents the ET reactivity fluctuation time, and the power-law exponent m_{dark} represents nonexponential distribution nature of the probability of the dark times. The τ determines the fluctuation time scale for a single molecule to shift from a bright state to a dark state statistically. Whereas, power-law exponent m_{dark} indicates the relative probability for the dark state duration: a larger m_{dark} suggests a relatively higher distribution probability for a shorter dart time states. As we have discussed above, the single-molecule fluorescence fluctuation as well as the dark states are due to the interfacial electron transfer dynamics fluctuation, and the longer a dark state lasts, the longer the interfacial electron transfer process dominates the ZnTCPP excited-state dynamics. Nevertheless, for a single-molecule fluorescence trajectory, the autocorrelation function decay time τ and the power-law exponent m_{dark} are critical factors for characterizing the ET reactivity in the ZnTCPP/TiO_2 system, and both parameters reveal the inhomogeneous fluctuation of the ET reactivity.

For a power-law distribution expressed as $P(t_{dark}) \propto t_{dark}^{-m_{dark}}$, the distribution is dominant by Lévy statistics at $1 < m_{dark} = 1 + \alpha < 2$:[85]

$$P(t_{dark}) \propto 1/t_{dark}^{1+\alpha}, 0 < \alpha < 1$$

Lévy statistics is usually observed in complex systems with nonlinear interactions, such as in physics and biology. Its typical characteristic is the diverging variance and a broad distribution expressed by power-law rule. In single-molecule spectroscopy, Lévy statistics has been extensively investigated in the blinking dynamics of quantum dots.[86−88] Some abnormal properties due to Lévy statistics, such as statistical aging and ergodicity breaking, have been deduced by calculating the evolution time of on (off) state or time-averaged correlation function or power spectra.[86,89]

Figure 6A shows that there are 21 power-law exponents met with $1 < m_{dark} < 2$, suggesting that the distribution of the dark states of 75% molecules examined obey Lévy statistics. We have calculated the evolution time of a ZnTCPP/TiO_2 system that spends in the dark states, that is, the total time spent in the dark state in the first N dark periods. For a single molecule trajectory, the evolution time of the dark state is defined as[86]

$$\theta(N) = \sum_{i=1}^{N} t_{dark}^{i}$$

where θ(N) is the total evolution time, and t_{dark} is the duration of a dark state and N is the state index in a single-molecule fluorescence intensity trajectory. Figure 7 shows the evolution time trace for two single-molecule trajectories with m_{dark} of 1.39 and 2.68. Obviously, the Lévy type evolution performs a nonlinear increase with N, and the sum $\theta(N)$ is almost dominated by few long-time events of the order of θ(N) itself, which unambiguously shows the diverging variance in Lévy statistics. The Lévy statistics of dark states quantitatively reveal the fluctuation mode of the interfacial ET reactivity in ZnTCPP/

(86) Brokmann, X.; Hermier, J. P.; Messin, G.; Desbiolles, P.; Bouchaud, J. P.; Dahan, M. *Phys. Rev. Lett.* **2003**, *90*, 120601-1–120601-4.
(87) Messin, G.; Hermier, J. P.; Giacobino, E.; Desbiolles, P.; Dahan, M. *Opt. Lett.* **2001**, *26*, 1891–1893.
(88) Barkai, E.; Jung, Y. J.; Silbey, R. *Annu. Rev. Phys. Chem.* **2004**, *55*, 457–507.
(89) Margolin, G.; Barkai, E. *J. Stat. Phys.* **2006**, *122*, 137–167.

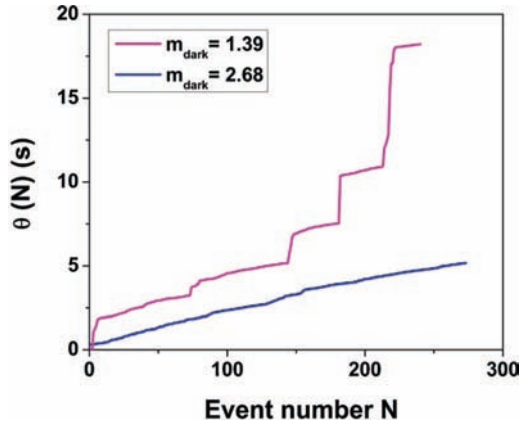

Figure 7. Evolution of total time spent in dark states $\theta(N)$ with the event index N. The curve with $m_{dark} = 1.39$, which obey Lévy statistics, shows rapid and nonlinear increase. The evolution is dominated by few events of the order of $\theta(N)$ itself.

TiO_2 system. We suggest that Lévy statistics of the interfacial ET can be ascribed to the complex interfacial site- and time-specific interactions between single ZnTCPP molecules and nanoscale local environments.[17,90]

Based on above discussion, we conclude that, for a single-molecule ZnTCPP/TiO_2 system, the interfacial ET reactivity usually fluctuates from time to time and from molecule to molecule, which display static and dynamic disorders in ET reactivity fluctuation dynamics. Power-law and autocorrelation function analysis based on the dark states are able to map the fluctuation of the single-molecule ET reactivity, and the interfacial ET reactivity of ZnTCPP/TiO_2 system can be quantitatively described by Lévy statistics.

The complex fluctuations of the interfacial electron transfer dynamics show characteristic dynamic disorder and static disorder.[3,18,72,74,75] We have attributed that the fluctuations are primarily originated from the FET rate fluctuation in a wide range across from ultrafast to ns and to even longer time scales. It is well-known that the interfacial electron transfer rate is highly sensitive to the molecular interactions between the adsorbed dye molecules and the TiO_2 substrate in a TiO_2-based dye sensitization system. The primary parameters of the molecular interaction are, for example, the electron transfer driving force of free energy gap between the excited-state of molecule and the conduction band of TiO_2 semiconductor, the vibrational relaxation energy of the adsorbed molecules and the surface vibrational modes of TiO_2, and the electronic coupling between the molecules and the TiO_2, etc. Among these parameters, the electronic coupling parameter is the most critical one on the interfacial FET rate from the excited-state of ZnTCPP to the conduction band of TiO_2. The inhomogeneous surface state distribution and specific surface states that in contact with the single-molecule ZnTCPP molecules play a critical role in the electronic coupling parameter. Specifically, the formation, stability and rupture of four dye−O−Ti−O−TiO_2 between the carboxylic groups of the ZnTCPP to TiO_2 may change and perturb electronic coupling significantly,[3,34] and the hydrogen bond interactions can be energetically perturbed by local environment thermal fluctuation at room temperature. Our conclusion is consistent with the ensemble-averaged measurements, which suggest that the origin of the inhomogeneity in interfacial ET can be ascribed to surface defects, electronic coupling, D−A distance, and multiple time scale of energetic relaxation and solvation dynamics.[91−93]

Previously, we have applied the electron-transfer resonant Raman spectroscopy to analyze the surface vibrational modes and the vibrational relaxation energies of the relevant molecular vibrational modes and the TiO_2 surface vibrational modes, and we have revealed that for alizarin/TiO_2 interfaces, a similar system to ZnTCPP/TiO_2, the vibrational reorganization energy barriers of interfacial electron transfer are inhomogeneous from TiO_2 nanoparticle to nanoparticle and from molecular site to site.[90] The broad inhomogeneity indicates that the vibronic interactions between the dye molecule and the TiO_2 substrate have a broad distribution of accessible energy states, which in turn gives a broad fluctuation subspace of the electronic coupling factors for a single-molecule interfacial electron transfer site on a TiO_2 nanoparticle surface. It is clear that more systematic experiments will be needed to completely identify and characterize the origins of the interfacial ET rate fluctuations at the ZnTCPP/TiO_2 system, although they are beyond the scope of this article, by controlling the surface electric potential to change the driving force, using single crystal TiO_2 rutile and anatase surfaces with controlled surface sites to examine the electronic coupling, and studying the single-molecule interfacial ET under different pH and temperature to identify the effect of the thermal motion on the single-molecule reactivity fluctuations.

Nevertheless, complex interfacial electron transfer dynamics has been reported over the last thirty years from ensemble-averaged experiments, and it is often that different electron transfer times (from fs to ns for FET time, and ns to ms for BET time) were reported for the same dye-sensitization system but from the different spectroscopy approach at different time resolutions.[51,52,58] Our observation of the static and dynamic disordered interfacial ET dynamics fluctuating across a wide time scale is consistent with the ensemble-averaged results and reveals partially the origin of the complexity of the interfacial ET dynamics.

Conclusion

We have studied the single-molecule interfacial ET dynamics in a ZnTCPP/TiO_2 nanoparticle system at room temperature, probing the fluorescence intensity fluctuation by single-molecule photon stamping recording each photon time delay from excitation, chronic arrival time, and specific phase associated with excitation laser polarization modulation. The ET occurrences are further demonstrated by single-molecule polarization and time-resolved control measurements, and the dark time in a single-molecule fluorescence fluctuation trajectory are identified to be originated from the duration when the forward electron transfer rate is higher than and dominated over the radiative decay rate of the excited-state of the adsorbed ZnTCPP molecule on a TiO_2 nanoparticle. The fluctuation of the electron transfer dynamics gives the single-molecule fluorescence fluctuation, and the dynamics of the fluorescence fluctuation reflects the single-molecule interfacial electron transfer dynamics fluctuation. The autocorrelation functions of the single-molecule fluctuation intensity trajectories show nonexponential decay, indicating the fluctuation dynamics involving an extended time scale from 10^{-2} to 10^2 s. The probability distributions of the

(90) Pan, D.; Hu, D.; Lu, H. P. *J. Phys. Chem. B* **2005**, *109*, 16390–16395.
(91) Bell, T. D. M.; Pagba, C.; Myahkostupov, M.; Hofkens, J.; Piotrowiak, P. *J. Phys. Chem. B* **2006**, *110*, 25314–25321.
(92) Murata, S.; Tachiya, M. *J. Phys. Chem. A* **2007**, *111*, 9240–9248.
(93) Bagchi, B.; Gayathri, N. *Adv. Chem. Phys.* **1999**, *107*, 1–80.

dark times from the single-molecule trajectories obey power-law rule, which represents a highly inhomogeneous and complex nature of the interfacial ET. On the basis of the power-law distribution analysis, the interfacial ET reactivity fluctuations of single molecules are identified to be predominately Lévy flight statistics. According this work and our previously reported work,[3,90] the highly inhomogeneous ET dynamics is most likely common for the interfacial chemical reactions that strongly regulated by the molecular interaction between adsorbed molecules and substrate surfaces. The spontaneous thermal fluctuations of the local environment and the molecular interactions occur at a wide time-scale at room temperature, resulting in the interfacial ET reaction-rate fluctuation and inhomogeneous dynamics. Our single-molecule spectroscopy analysis provides detailed information about the inhomogeneity of the interfacial electron transfer, which is consistent but not obtainable from the conventional ensemble-averaged experiments.

Acknowledgment. This work is supported by the Office of Basic Energy Sciences within the Office of Science of the U.S. Department of Energy (DOE).

JA806988D